Substrate Optimization for Integrated Circuit Antennas

NICOLAOS G. ALEXOPOULOS, SENIOR MEMBER, IEEE, PISTI B. KATEHI, STUDENT MEMBER, AND D. B. RUTLEDGE, MEMBER, IEEE

Abstract—**The reciprocity theorem and integral equation techniques are employed to determine the properties of integrated-circuit antennas. The effect of surface waves is considered for dipole and slot elements on substrates. The radiation and bandwidth of microstrip dipoles are optimized in terms of substrate thickness and permittivity.**

I. INTRODUCTION

INTEGRATED OR printed circuit antennas are a natural evolution of integrated circuit components in the microwave as well as millimeter-wave frequencies. In both frequency ranges various metallization geometries have been developed pertinent to specific antenna performance requirements. In microwave, printed rectangular or circular patches, as well as microstrip dipoles and variations thereof, are the most popular elements [1]–[6], while in millimeter waves, slots [7], dipole arrays [8], slot arrays [9]–[11], Vees [12] and microstrip patches [13]–[15] have been developed.

The many advantages of printed circuit antennas (such as low weight, conformality to a given surface, low cost, and ease of hybrid and monolithic integration) are often counterbalanced by low element gain, very narrow bandwidth, and limited power. Power is limited by the thermal capacity of the substrate materials, but the gain can be improved by constructing arrays. Furthermore, the printed circuit antenna characteristics such as radiation, efficiency, bandwidth, input and mutual impedance, and radiation pattern can be optimized by a judicious choice of substrate thickness and relative permittivity value. It is well known that dielectric substrates are excellent surface waveguides [16]–[18] with a fundamental mode with no cutoff. For this reason, an optimization of the printed circuit antenna properties requires a careful analysis of the antenna as a source of surface waves in the substrate.

This paper is devoted to the examination of how the substrate thickness and permittivity parameters can be optimized so as to yield improved antenna characteristics. The structures which have been investigated are (see Fig. 1) (a) elementary (infinitesimally short) dipole excitation of a dielectric substrate, (b) elementary slot excitation, and (c) microstrip dipole (resonant or arbitrary length) excitation. In the former two cases the reciprocity theorem [19], [20] is invoked to calculate the power in the surface modes, as well as the radiated field and gain of elementary dipoles and slots, while in the latter case an integral equation approach has been applied to yield a tradeoff analysis for resonant length microstrip dipoles. The important antenna characteristics can be obtained by numerical solution of the integral equation for the antenna current distribution. Furthermore, this approach enables the determination of the substrate thickness for which the optimum radiation efficiency and bandwidth can be obtained.

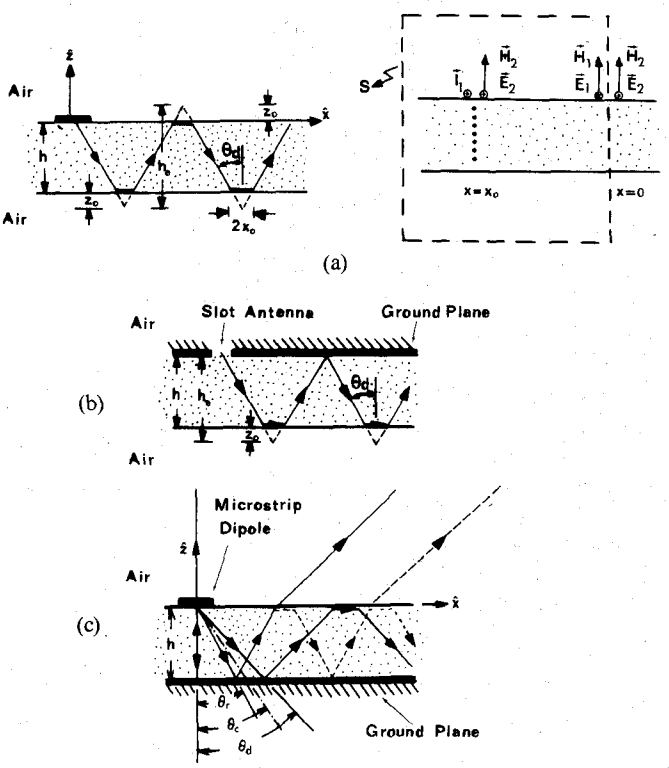

Fig. 1. Dipole and slot antennas on substrate.

II. APPLICATION OF THE RECIPROCITY THEOREM TO ELEMENTARY DIPOLES AND SLOTS

The power carried in surface-wave modes, radiated power, and gain of elementary printed circuit antennas are computed in this section with the aid of the Lorentz reciprocity theorem which states that for the two sets of current density sources $\bar{J}_1$ or $\bar{J}_2$ [19], [20] (which oscillate at

Manuscript received October 6, 1982; revised February 18, 1983. This work was supported in part by the U.S. Navy under Contract N00014-79-C-0856, in part by the U.S. Army under Contract DAAG 29-79-C-0050, and in part by the Department of Energy under Contract DE-AT03-76ETS53019, TASK IIIB.

N. G. Alexapoulos and P. B. Katehi are with the Electrical Engineering Department, University of California, Los Angeles, CA 90024.

D. B. Rutledge is with the Division of Engineering and Applied Science, California Institute of Technology, Pasadena, CA 91125.

0018-9480/83/0700-0550$01.00 ©1983 IEEE

a common frequency) the generated fields $(\bar{E}_1, \bar{H}_1)$ and $(\bar{E}_2, \bar{H}_2)$ satisfy over a region V enclosed by a surface S the following relationship:

$$\int_S [\bar{E}_1 \times \bar{H}_2 - \bar{E}_2 \times \bar{H}_1] \cdot \overline{dS} = \int_V [\bar{E}_2 \cdot \bar{J}_2 - \bar{E}_1 \cdot \bar{J}_1]\, dV. \quad (1)$$

The analysis is carried out by considering the TM and TE structure of the propagating modes and a ray picture which accounts for the effective substrate thickness and the Goos-Hänchen shift [18]. The ray picture pertinent to the elementary printed dipole and slot elements is shown in Fig. 1. The effective substrate thickness for an ungrounded slab is $h_e = h + 2z_0$, where h is the actual thickness and z_0 the apparent ray penetration depth. For a grounded slab we have $h_e = h + z_0$. In terms of h_e, the power per unit width in a surface wave is given by [18] $P = EHh_e/4$, where E and H are the maximum transverse field amplitudes.

A. Surface Wave Power by Reciprocity

Application of the reciprocity theorem to the computation of surface-wave power has been considered in a two-dimensional setting [17]. The analysis is extended here to consider elementary printed dipoles on a substrate and slots in a ground plane with a substrate. In this case, the reciprocity theorem is applied to the current element and a surface-wave mode. It is determined that the power coupled into a surface-wave mode is given by simple formulas with the guide effective thickness h_e for the given mode always in the denominator.

The calculation for TE surface-wave modes, where the excitation is provided by an electric current element as shown in Fig. 1(a) is now sketched briefly. The current element $\bar{I}_1$ at x_0 produces the surface-wave field $\bar{E}_1, \bar{H}_1$ at $y = 0$. A second surface-wave field $\bar{E}_2, \bar{H}_2$ is assumed to propagate from right to left and it is normally incident on the current element. The Lorentz reciprocity theorem applied to a large box S (see Fig. 1(a)) yields the surface-wave power per unit width, normal to the current element, as

$$P_{\text{normal}} = \frac{3\lambda_0 \cos^2 \phi_{\text{TE}}}{4h_e \pi x_0} \quad (2)$$

where h_e is the effective guide thickness. Details of the calculation as well as other examples are given in [33], where it is assumed that $x_0 \gg \lambda_0$ and where ϕ_{TE} is found in Kogelnik [18]. This power is normalized to the power the element would radiate in vacuum. The power is maximum in this direction and varies as the square of the cosine of the angle from the normal. The total power in the TE surface-wave mode is found to be

$$P^{\text{TE}}_{\text{dipole}} = \frac{3\lambda_0 \cos^2 \phi_{\text{TE}}}{4h_e}. \quad (3)$$

In contrast, the power in a TM mode is maximum along the current element axis, and is given by

$$P_{\text{axial}} = \frac{3\lambda_0 \sin^2 \phi_{\text{TM}} \cos^2 \theta_d}{4h_e \pi x_0} \quad (4)$$

where θ_d is the propagation angle within the guide (see Fig. 1(a)). In this case, the total power is

$$P^{\text{TM}}_{\text{dipole}} = \frac{3\lambda_0 \sin^2 \phi_{\text{TM}} \cos^2 \theta_d}{4h_e} \quad (5)$$

where ϕ_{TM} is also given by Kogelnik [18]. Similar calculations give the power coupled into surface-wave modes by an infinitesimal slot in a grounded substrate. For a slot, the maximum power density for the TM modes is normal to the slot, while for TE modes it is parallel to it. The total power normalized to the power the slot would radiate in free space is given by

$$P^{\text{TM}}_{\text{slot}} = \frac{3\epsilon_r \lambda_0}{16h_e} \quad (6)$$

and

$$P^{\text{TE}}_{\text{slot}} = \frac{3\epsilon_r \lambda_0 \cos^2 \theta_d}{16h_e} \quad (7)$$

where θ_d is shown in Fig. 1(b). These expressions have been computed and the numerical results are presented in graphical form in Fig. 2. Fig. 2 shows results for $\epsilon_r = 4$ (quartz) and $\epsilon_r = 12$ (appropriate for silicon or GaAs).

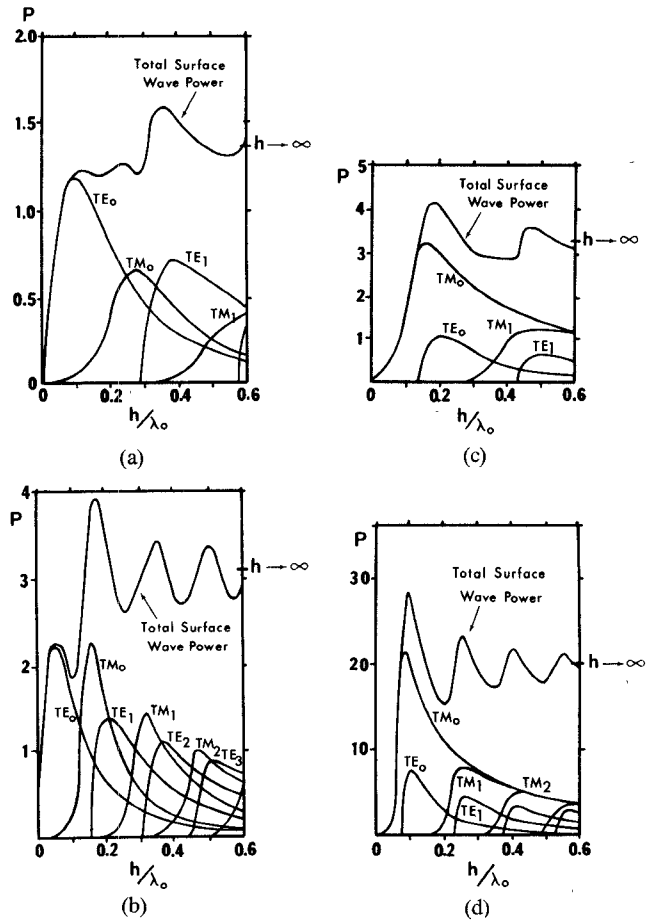

Fig. 2. Normalized power versus substrate thickness. (a) Dipole on quartz substrate. (b) Dipole on silicon or GaAs substrate. (c) Slot on quartz substrate. (d) Slot on silicon or GaAs substrate.

The results for dipoles show that, as the substrate thickness increases, the normalized surface-wave power becomes quickly larger than unity. The power in surface-wave modes is small only when $h \ll \lambda_0/10$. As h increases, the power in individual modes rises and falls but the total power is a

damped oscillation. In addition, it is observed that TE modes "turn on" much more quickly than TM modes. The corresponding results for slots are also shown in Fig. 2 and they are seen to be qualitatively similar to those of printed dipoles. However, the surface-wave power does not increase quickly for small h, because there is no TE_0 mode on the grounded substrate. The normalized surface-wave power for thick substrates is larger than the corresponding power for the dipole elements.

The limit of total surface-wave power for large h can also be calculated. For the electric dipole, it is given by [21]

$$P_{\text{dipole}}^{\text{surface wave}} = \frac{1}{\epsilon_r+1}\left[\frac{1}{2}\left(1+2\epsilon_r+\frac{3\epsilon_r}{\epsilon_r^2-1}\right)\left(\sqrt{\epsilon_r-1}\right) - \frac{\epsilon_r^2 \ln\left(\epsilon_r+\sqrt{\epsilon_r^2-1}\right)}{\frac{2}{3}(\epsilon_r-1)(\epsilon_r+1)^{3/2}}\right] \tag{8}$$

and it is observed that as ϵ_r increases, the power approaches $\sqrt{\epsilon_r}$ asymptotically. The corresponding formula for the slot can be calculated as the power emitted by a magnetic current element on a ground plane at angles larger than the critical angle. We find that the surface-wave power is given by

$$P_{\text{slot}}^{\text{surface wave}} = \frac{\epsilon_r}{2}\left(\sqrt{\epsilon_r-1}\right) - \frac{\sqrt{\epsilon_r-1}}{8}. \tag{9}$$

Here, as ϵ_r increases, the power tends to the asymptotic value of $\frac{1}{2}(\epsilon_r)^{3/2}$. Expressions (8) and (9) are shown graphically in Fig. 3 and are plotted in Fig. 2 for $\epsilon_r = 4$ and 12.

B. Radiated Power by Reciprocity

In this section, the reciprocity theorem is applied for the calculation of radiated power. The approach is an extension of [32] and details are omitted. The analysis involves an equivalent transmission-line model [19] to include the effect of the substrate. Thus, a normalized wave impedance is defined as

$$\eta = \begin{cases} \dfrac{\cos\theta_1}{\sqrt{\epsilon_r}\cos\theta_0}, & \text{TM waves} \\ \dfrac{\cos\theta_0}{\sqrt{\epsilon_r}\cos\theta_1}, & \text{TE waves} \end{cases} \tag{10}$$

where θ_0 is the angle in the air and θ_1 the refracted angle, as calculated by Snell's law, in the substrate. The following auxiliary quantities are now defined:

$$A_i \equiv \cos^2\psi + \eta^2 \sin^2\psi \tag{11}$$

and

$$B_i \equiv \cos^2\psi + \left(\frac{\eta+\eta^{-1}}{2}\right)^2 \sin^2\psi \tag{12}$$

where $i=1$ for TE and $i=2$ for TM waves, and ψ is the electrical substrate thickness, given by

$$\psi = 2\pi\sqrt{\epsilon_r}\, h \cos\theta_1/\lambda_0. \tag{13}$$

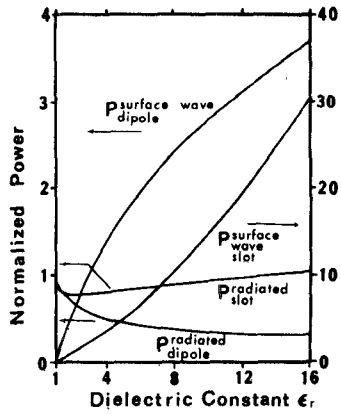

Fig. 3. Normalized power versus ϵ_r.

The power radiated down through the substrate is

$$P_{\text{dipole}}^{\text{down}} = \frac{3}{8}\int_0^1 \left[\frac{1}{B_1}+\frac{u^2}{B_2}\right] du \tag{14}$$

and

$$P_{\text{slot}}^{\text{down}} = \frac{3}{8}\int_0^1 \left[\frac{u^2}{A_1}+\frac{1}{A_2}\right] du \tag{15}$$

while the power radiated up into the air is

$$P_{\text{dipole}}^{\text{up}} = \frac{3}{8}\int_0^1 \left[\frac{A_1}{B_1}+u^2\frac{A_2}{B_2}\right] du \tag{16}$$

where $u = \cos\theta_0$. The power radiated by the infinitesimal slot up into the air is precisely the same as it would be without the substrate, i.e., the ground plane effectively isolates the power going up from the power going down. In terms of normalized power we just have

$$P_{\text{slot}}^{\text{up}} = \frac{1}{2} \tag{17}$$

independent of substrate thickness and dielectric constant. Fig. 4 shows the radiated power for (a) dipoles and (b) slots and it is observed that the power coupled into surface-wave modes is almost always larger than the power radiated in air. It is also seen that the radiated dipole power exhibits sharp peaks when the thickness is a multiple of a half-dielectric wavelength, while the peaks for the corresponding slot element case occur at odd multiples of a quarter wavelength. These results, together with those exhibited in Figs. 2 and 3, indicate that surface-wave power dominates the radiated power except for very thin substrates.

The limit for the total radiated power can also be computed for dipoles and slots for large h. For dipoles the result can be obtained [21] as

$$P_{\text{dipole}}^{\text{radiated}} = \frac{1}{(\epsilon_r+1)}\left\{\frac{\epsilon_r^{5/2}-1}{\epsilon_r-1}+\frac{\epsilon_r}{2\left(\sqrt{\epsilon_r}+1\right)}\left(1-\frac{3\sqrt{\epsilon_r}}{\epsilon_r+1}\right) + \frac{\epsilon_r^2 \ln\left(\sqrt{\epsilon_r+1}-\sqrt{\epsilon_r}\right)\left(\sqrt{\epsilon_r}+1\right)/\sqrt{\epsilon_r}}{2/3(\epsilon_r+1)^{3/2}(\epsilon_r-1)}\right\} - P_{\text{dipole}}^{\text{surface wave}}. \tag{18}$$

Similarly, the power radiated by the slot can be obtained

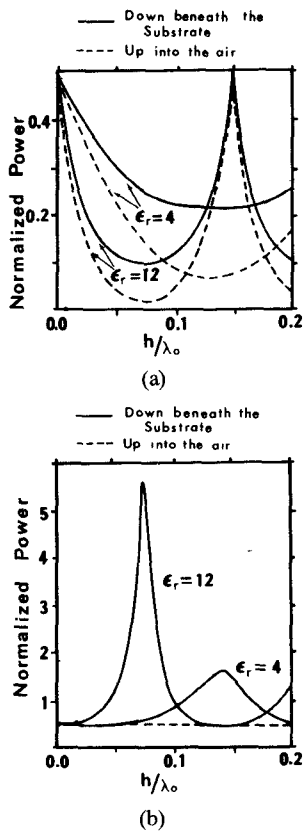

Fig. 4. Normalized radiated power for (a) printed dipoles and (b) slots.

by integrating the power emitted by the slot at angles smaller than the critical angle. By adding the result $P_{\text{slot}}^{\text{up}} = 1/2$, the following expression is obtained:

$$P_{\text{slot}}^{\text{radiated}} = \frac{\epsilon_r^{3/2}+1}{2} - P_{\text{slot}}^{\text{surface wave}}. \tag{19}$$

These formulas have been plotted in Fig. 3. It is again observed that surface-wave power dominates the radiated power, particularly with increasing ϵ_r.

C. Gain of Elementary Dipoles and Slots on Substrates

In most near-millimeter systems, the antennas would act as feed antennas for a lens or mirror. In order to be an efficient feed antenna, the beam should be concentrated in the direction of the lens or mirror. The required gain depends on the system, but generally speaking, a gain of 5 (7 dB) or higher is desirable. The data provided in Figs. 2 and 4 yield, with additional calculations, the gain normal to the substrate. The gains are plotted in Fig. 5. The gain is almost always larger down through the substrate. Even in this direction, however, the dipole gain falls off very rapidly from 1.5 at zero thickness to 1 at $0.008\lambda_0(\epsilon_r = 12)$ and $0.035\lambda_0(\epsilon_r = 4)$. For slots, the gain hovers briefly about 1.5 and then falls to 1 at $0.01\lambda_0(\epsilon_r = 12)$ and $0.14\lambda_0(\epsilon_r = 4)$. In no case would these antennas alone make adequate feed antennas. In a practical system, the antennas would be resonant half-wave dipoles or slots rather than elementary dipoles and slots. In general, however, the patterns for the resonant antennas do not differ greatly from those of the elementary antennas. These gain graphs should be suitable

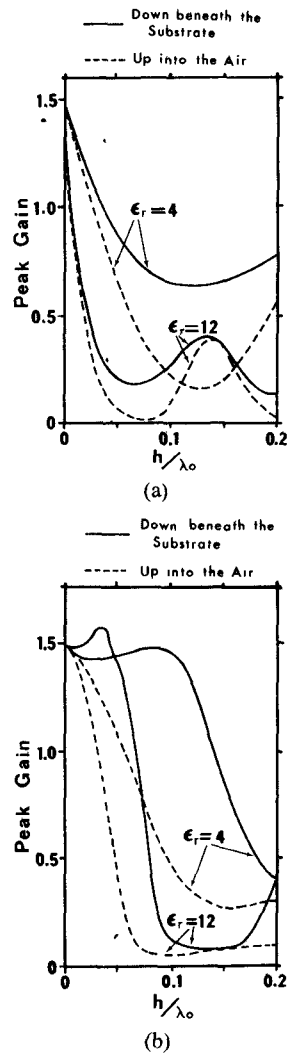

Fig. 5. Peak gain versus substrate thickness. (a) Gain for printed dipoles. (b) Gain for slots.

as design guides for the resonant antennas, for which calculations are more difficult. The data show that the surface waves must be considered, and that these antennas must be modified, either as a microstrip antenna, an array [8]–[10], or a lens-coupled antenna [11] to make an adequate feed.

III. Integral Equation Solution—Finite Length Microstrip Dipoles

The results presented for infinitesimally short dipoles and slots shed information as to the basic behavior of elementary antennas on dielectric substrates. These results also led to the conclusion that neither the printed dipole nor the slot on a ground plane on a substrate are effective feed antennas. A fruitful direction is that of microstrip antennas and in this section microstrip dipoles will be considered with the aim being to optimize the radiation properties of the printed circuit element. Since practical microstrip dipoles are of finite length, it is important to be able to compute the antenna resonant length L_r, radiation efficiency η, and bandwidth BW, as well as input impedance. The aim here is to emphasize the impact of substrate thickness and relative permittivity on the antenna parame-

ters L_r, η, and BW. To this end, the Pocklington [23] integral equation for the antenna current distribution is solved by employing the method of moments [24], [25]. The pertinent integral equation in this case is

$$\bar{E}(x,y,z) = \iint \left[k_0^2 \bar{\bar{I}} + \nabla\nabla\right] \cdot \bar{\bar{G}}(\bar{r}/\bar{r}') \cdot \bar{J}(\bar{r}')\, ds' \quad (20)$$

where the integration is carried over the metallization area occupied by the antenna. Furthermore, in (20), $\bar{\bar{I}}$ is the idemfactor or unit dyadic, i.e., $\bar{\bar{I}} = \hat{x}\hat{x} + \hat{y}\hat{y} + \hat{z}\hat{z}$, $\bar{J}(\bar{r}')$ is the current density distribution on the antenna and $\bar{\bar{G}}(\bar{r}/\bar{r}')$ is the dyadic Green's function obtained for an elementary printed dipole on a grounded substrate [24]–[30]. By considering for simplicity the microstrip antenna to be a printed linear dipole in the x-direction, (20) reduces to [28], [29]

$$E_x = \int_0^L \left[k_0^2 G_x + \frac{\partial^2}{\partial x^2}(G_x - G)\right] J_x\, dx' \quad (21)$$

where L is the dipole length and

$$G_x = -\frac{j\omega\mu_0}{2\pi k_0^2}(1-\epsilon_r) \cdot \int_0^\infty J_0(\zeta\rho)\left\{\frac{\sinh(uh)}{F_1(\zeta,h)}\right\}\left\{\frac{\sinh(uh)}{F_2(\zeta,h)}\right\} u\zeta\, d\zeta \quad (22)$$

$$G = \frac{j\omega\mu_0}{2\pi k_0^2}(1-\epsilon_r) \cdot \int_0^\infty J_0(\zeta\rho)\left\{\frac{\sinh(uh)}{F_1(\zeta,h)}\right\}\left\{\frac{\cosh(uh)}{F_2(\zeta,h)}\right\} u_0\zeta\, d\zeta \quad (23)$$

with

$$F_1(\zeta,h) = u_0 \sinh(uh) + u\cosh(uh) \quad (24)$$

$$F_2(\zeta,h) = \epsilon_r u_0 \cosh(uh) + u\sinh(uh) \quad (25)$$

$$\rho = \sqrt{(x-x')^2 + (y-y')^2}^{1/2} \quad (26)$$

and

$$u_0 = \sqrt{\zeta^2 - k_0^2}^{1/2} \quad u = \sqrt{\zeta^2 - k^2}^{1/2} \quad k = \sqrt{\epsilon_r}\, k_0. \quad (27)$$

A careful investigation of $F_1(\zeta,h)$ and $F_2(\zeta,h)$ shows that their zeros lie in the range $k_0 < \zeta < k$ and that they correspond to the TM, TE types of surface-wave modes, respectively. The number of modes that propagate for a given ϵ_r and h is [24]

TM modes:

$$N_{\mathrm{TM}} = n+1 \quad n\pi < \nu < (n+1)n, \quad n = 0,1,2,3\cdots$$

TE modes:

$$N_{\mathrm{TE}} = \begin{cases} 0, & \nu < \pi/2 \\ n, & (n-1/2)\pi < \nu < (n+1/2)\pi, \quad n = 1,2,3,\cdots \end{cases}$$

where $\nu = \sqrt{\epsilon_r - 1}\, k_0 h$.

In order to solve the integral equation for the antenna current distribution, the method of moments has been adopted with piece-wise continuous sinusoidal functions [24]–[26] being the basis set of expansion functions. Furthermore, it has been assumed that the dipoles are center-fed, and special integration methods have been developed [24]–[26] to evaluate the Sommerfeld type integrals of (22)–(23).

A. Radiation Efficiency

With the assumption that the dipoles are center-fed with a unit voltage excitation, the input impedance is computed from $Z_{\mathrm{in}} = V/I(0)$, where $I(0)$ is the current value at the microstrip dipole input terminals. From these computations the resonant length and resonant input resistance are extracted. Furthermore, the resonant imput resistance R_r consists of the surface-wave resonant resistance R_{rs} and the radiation resonant resistance R_{rr}, i.e., $R_r = R_{rs} + R_{rr}$, since R_{rs} and R_{rr} are directly proportional to the power coupled into the substrate as guided modes and to the power radiated in space, respectively. The radiation efficiency of the microstrip dipole is defined as (at resonance)

$$\eta = \frac{R_{rr}}{R_{rr} + R_{rs}} \quad (28)$$

where dielectric substrate and antenna conductor losses have been omitted. The variation of R_{rs}, R_{rr}, and R_r with respect to substrate thickness h is shown in Fig. 6 for PTFE glass ($\epsilon_r = 2.17$), quartz ($\epsilon_r = 4.0$), and GaAs ($\epsilon_r \simeq 12.5$). For each case, the guided mode distribution in the substrate is also shown in Fig. 6, and a close scrutiny of these results indicates that the maximum radiation efficiency is obtained at the cutoff thickness of the TE_0 mode in the substrate. This has been verified to be the case for any given ϵ_r and, in addition, as ϵ_r increases, η obtains maxima at the TE_n mode and minima at the TM_n mode cutoff thickness (see Fig. 6(c)). The optimum substrate thickness h_0 for maximum radiation efficiency η_0 is shown in Fig. 7 for varying ϵ_r with the corresponding microstrip dipole resonant length also superimposed. This figure indicates that if a maximum radiation efficiency of better than 50 percent is desired the substrate relative permittivity should be $\epsilon_r \lesssim 4.5$ with a resulting substrate thickness $h_0 \gtrsim 0.15\lambda_0$ and a dipole resonant length $L_r \gtrsim 0.25\lambda_0$.

The phenomenon of the optimum radiation efficiency occurring just before the TE_0 surface-wave mode is excited in the substrate can be explained by considering Figs. 1(c) and 8. Fig. 8 shows a printed electric dipole, the direction of propagation of the TM and TE surface-wave modes, and the polarization of the electric field radiated by the dipole inside the substrate and in air (solid lines). If the ray picture of Fig. 1(c) is referred to, it is observed that all rays with $\theta > \theta_c$ ($\theta_c \equiv$ critical angle) are trapped as guided substrate modes. Those rays with $\theta < \theta_c$ undergo a reflection at the ground plane with a 180° phase shift and after refracting at the substrate–air interface contribute to the radiation field. The TM refracted rays (dashed lines) mostly add in phase to while the TE refracted rays (dashed lines) mostly cancel out the directly radiated rays. Thus, since the TM_0 mode has zero cutoff and is launched more efficiently as the substrate thickness increases, it adds more energy to the radiated field, thus increasing the radiation efficiency. When the TE_0 mode is excited, the radiation efficiency decreases since the TE_0 mode refracted rays mostly cancel

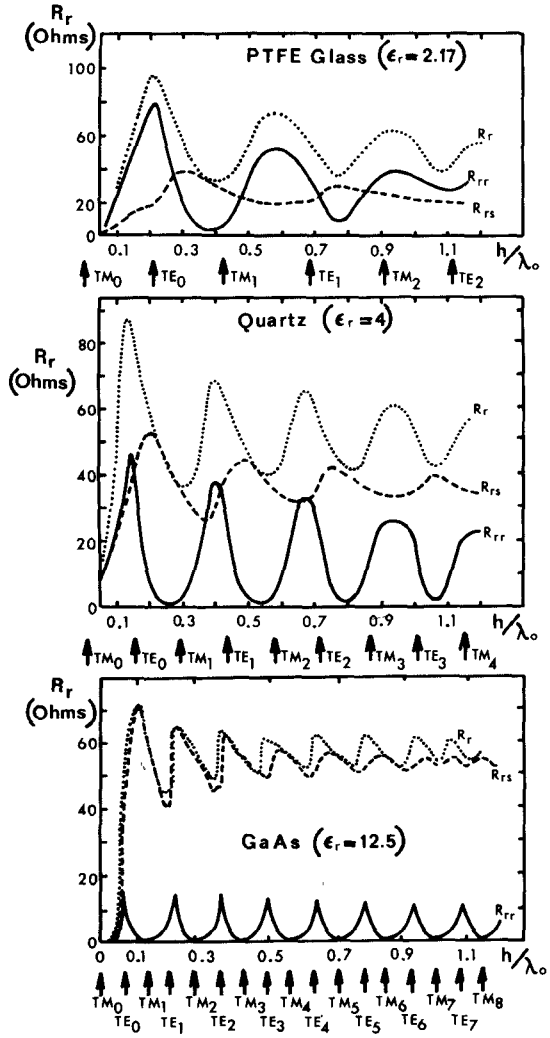

Fig. 6. Resonant resistance versus substrate thickness.

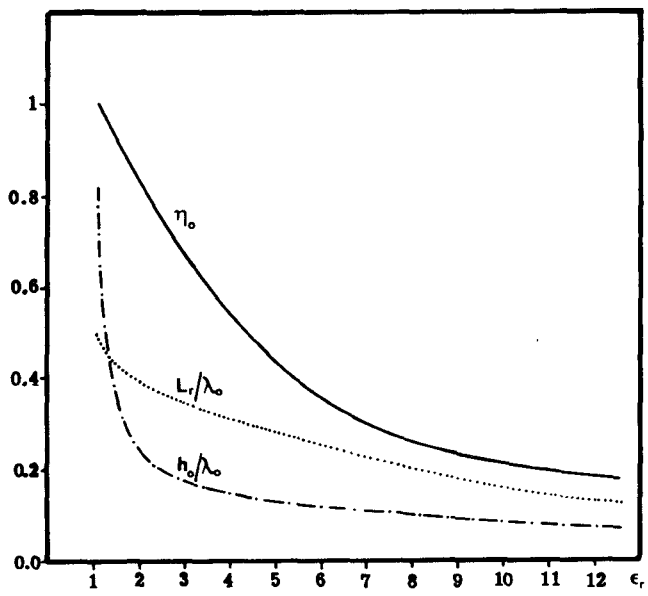

Fig. 7. Optimum radiation efficiency versus ϵ_r.

out the directly radiated field. As the substrate thickness increases and additional TM_n and TE_n surface-wave modes are excited, the minima and maxima of η do not coincide with the cutoff points of the TM_n and TE_n modes ($n > 0$)

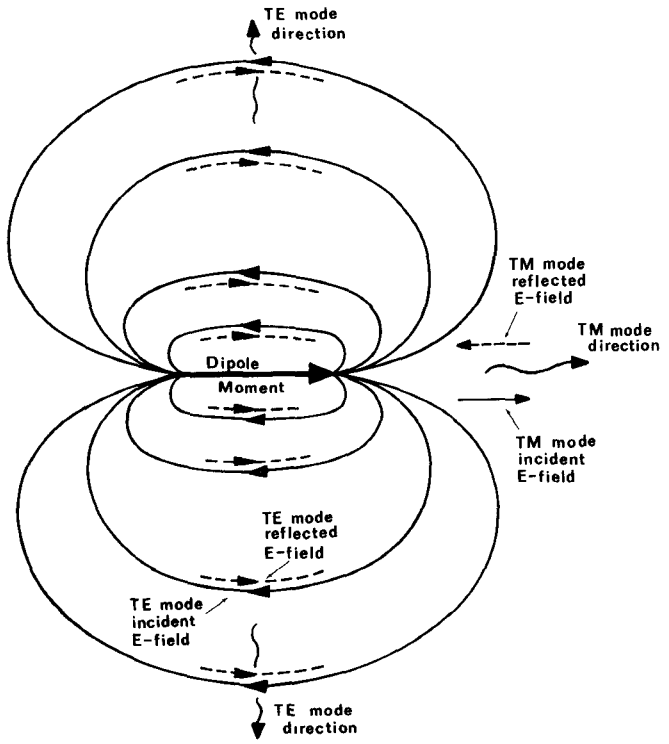

Fig. 8. Radiation mechanism by a microstrip dipole.

as the refracted rays of these modes undergo phase shifts at the substrate–air interface, which are neither in nor out of phase. As the substrate relative permittivity increases, however, the TM_n refracted rays add in phase while the TE_n refracted rays add out of phase with the radiated field, and therefore the minima and maxima of η coincide with the respective cutoff thickness of these modes (see Fig. 6(c)).

B. Resonant Length

In many practical situations, an antenna input impedance of 50 Ω is necessary. Under such circumstances a design can be pursued by utilizing Fig. 6 to determine the substrate thickness. The length of the microstrip dipole can be inferred from Fig. 9 where the antenna resonant length has been presented versus substrate thickness h. Here it is obvious that, as expected, L_r decreases as ϵ_r increases, and as h increases without bound, L_r approaches the value of the resonant length of a dipole printed on a dielectric half-space.

C. Bandwidth

It is well known that microstrip antennas have very small bandwidth [1]. It is possible, however, to improve bandwidth performance by optimizing substrate properties (it is assumed that antenna geometry is fixed). This will be demonstrated here for the substrate materials under consideration, for the case of printed circuit dipoles. In terms of the parameters discussed up to now bandwidth can be defined as

$$\mathrm{BW} = \frac{1}{L_r} \frac{2R_r}{\left.\dfrac{dX_{\mathrm{in}}}{dL_\lambda}\right|_{L_r}} \tag{29}$$

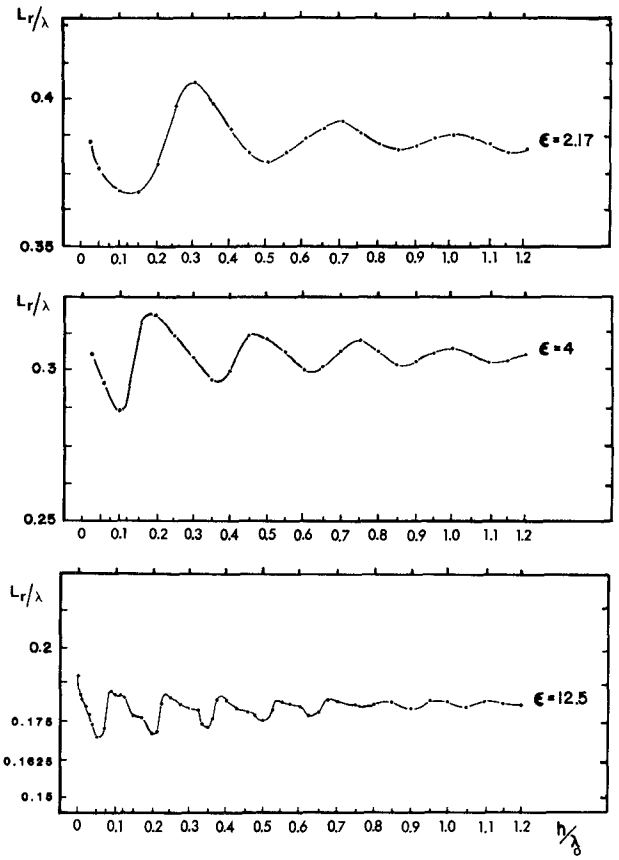

Fig. 9. Resonant length L_r versus substrate thickness h (in λ_0).

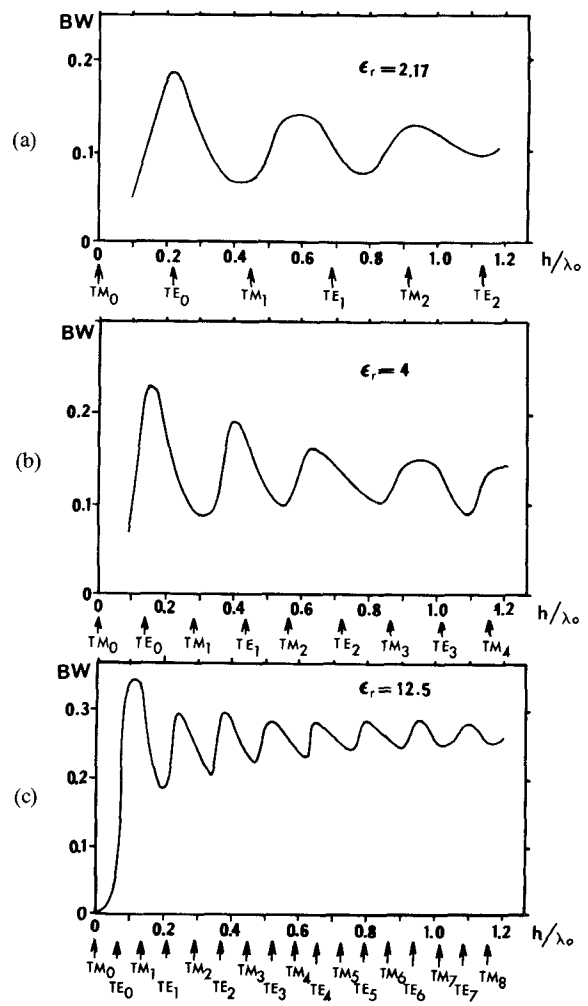

Fig. 10. Bandwidth BW versus h/λ_0.

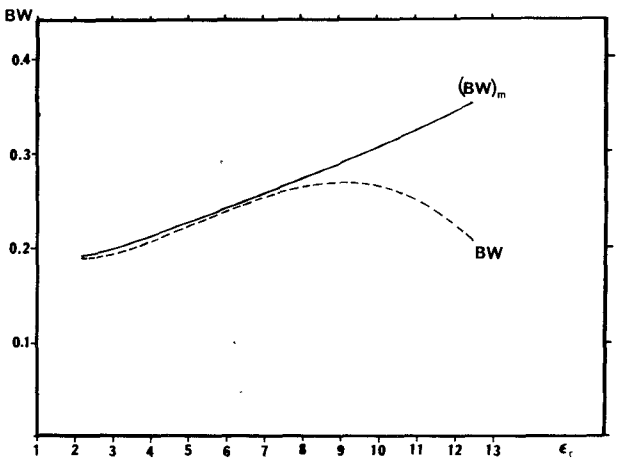

Fig. 11. Bandwidth versus ϵ_r. $(BW)_m$ = Maximum bandwidth. BW = Bandwidth corresponding to optimum radiation-efficiency substrate thickness.

where $L_\lambda = L/\lambda$, and dX_{in}/dL_λ is the derivative of the input reactance with respect to antenna length normalized to wavelength in the dielectric. This derivative is evaluated at the resonant length of the input impedance. The variation of BW with h is shown in Fig. 10, where it is observed that the maximum occurs at a thickness beyond the cutoff of the TE_0 mode. Fig. 11 depicts the variation of BW with respect to the substrate permittivity ϵ_r. It is observed in this figure that the maximum bandwidth $(BW)_m$ increases monotonically with ϵ_r, whereas the bandwidth BW for a substrate thickness corresponding to optimum radiation efficiency reaches a maximum value of approximately 26 percent when $\epsilon_r \simeq 9.4$, and thereafter it decreases monotonically.

IV. Conclusions

In this paper, the effect of the substrate on printed-circuit antennas has been considered. It is found that the gain of elementary dipoles and slots is reduced because of surface-wave excitation. This indicates that the corresponding resonant single antennas will not make adequate feeds.

Microstrip dipoles have more favorable characteristics for several reasons. They radiate in only one direction. The lowest order TE mode that limits the dipole on an ungrounded substrate is cutoff, and the dipole does not excite the TM_0 mode as strongly as the slot does. Microstrip dipoles have been analyzed in this paper by employing numerical techniques (method of moments) to solve Pocklington's integral equation for the antenna current distribution. From these computations, pertinent information has been extracted as to the effect of substrate properties on microstrip dipole resonant length, input resonant resistance, radiation efficiency, and bandwidth. It has been determined that optimum radiation efficiency is obtained when the substrate thickness is chosen at the cutoff thickness of the TE_0 mode. Furthermore, it has been shown that the substrate relative permittivity must be less than $\epsilon_r \lesssim 4.5$

if a radiation efficiency of better than 50 percent is desired. Bandwidth has been found to be maximum beyond the TE_0 substrate thickness cutoff and to increase monotonically with increasing ϵ_r. On the other hand, it has been shown that the bandwidth obtained for a substrate thickness which correspond to the optimum radiation efficiency substrate thickness reaches a maximum BW $\simeq$ 27 percent at about $\epsilon_r \simeq 9.4$.

REFERENCES

[1] K. R. Carver and J. W. Mink, "Microstrip antenna technology," *IEEE Trans. Antennas Propagat.*, vol. AP-29, pp. 2–24, Jan. 1981.

[2] R. J. Mailloux, J. F. McIlvenna, and N. P. Kernweis, "Microstrip array technology," *IEEE Trans. Antennas Propagat.*, vol. AP-29, pp. 25–27, Jan. 1981.

[3] W. F. Richards, Y. T. Lo, and D. D. Harrison, "An improved theory for microstrip antennas and applications," *IEEE Trans. Antennas Propagat.*, vol. AP-29, pp. 38–46, Jan. 1981.

[4] D. C. Chang, "Analytical theory of an unloaded rectangular microstrip patch," *IEEE Trans. Antennas Propagat.*, vol. AP-29, pp. 54–62, Jan. 1981.

[5] T. Itoh and W. Menzel, "A full-wave analysis method for open microstrip structures," *IEEE Trans. Antennas Propagat.*, vol. AP-29, pp. 63–68, Jan. 1981.

[6] H. G. Oltman and D. H. Huebner, "Electromagnetically coupled microstrip dipoles," *IEEE Trans. Antennas Propagat.*, vol. AP-29, pp. 151–157, Jan. 1981.

[7] B. J. Clifton, R. A. Murphy, and G. D. Alley, "Integrated monolithic mixers on GaAs for millimeter and submillimeter wave applications," in *Conf. Dig. 4th Int. Conf. Infrared and Millimeter Waves and their Applications*," IEEE Cat. no. 79CH1384-7 MTT, 1979, pp. 84–86.

[8] P. T. Parrish, T. C. L. G. Sollner, R. H. Mathews, H. R. Fetterman, C. D. Parker, P. E. Tannenwald, and A. G. Cardiasmenos, "Printed dipole Schottky diode millimeter wave antenna array," in *SPIE Proc.*, 1982, vol. 337-30.

[9] A. R. Kerr, P. H. Siegel, and R. J. Mattauch, "A simple quasi-optical mixer for 100–120 GHz," in *1977 IEEE MTT-S Int. Microwave Symp. Dig.*, pp. 96–98.

[10] L. Yuan, J. Paul, and P. Yen, "140 GHz quasi-optical planar mixers," in *1982 IEEE MTT-S Int. Microwave Symp. Dig.*, pp. 374–375.

[11] D. P. Niekirk, D. B. Rutledge, M. S. Muha, H. Park, and C. -X. Yu, "Far infrared imaging antenna arrays," *Appl. Phys. Lett.*, vol. 40, pp. 203–205, Feb. 1, 1982.

[12] T. L. Hwang, D. B. Rutledge, and S. E. Schwarz, "Planar sandwich antennas for submillimeter applications," *Appl. Phys. Lett.*, vol. 34, pp. 9–11, Jan. 1, 1979.

[13] P. Hall *et al.*, "Feasibility of designing millimeter microstrip planar antenna arrays," in *AGARD Conf. Proc. 245, Millimeter and Submillimeter Wave Propagation and Circuitry*, Sept. 1978.

[14] M. Weiss, "Microstrip antennas for millimeter waves," Tech. Rep. ECOM 76-0110, Oct. 1977.

[15] M. Weiss and R. Cassel, "Microstrip millimeter wave antenna study," Tech. Rep. CORADCOM-77-0158F, Apr. 1979.

[16] R. E. Collin, *Field Theory of Guided Waves*. New York: McGraw-Hill, 1960.

[17] C. H. Walter, *Traveling Wave Antennas*. New York: McGraw-Hill, 1965, pp. 290–299.

[18] H. Kogelnik, "Theory of dielectric waveguides," in *Integrated Optics*, T. Tamir, Ed. New York: Springer-Verlag, 1975.

[19] R. F. Harrington, *Time-Harmonic Electromagnetic Fields*. New York: McGraw-Hill, 1961.

[20] R. S. Elliott, *Antenna Theory and Design*. Englewood Cliffs, NJ: Prentice-Hall, 1981, pp. 39–41.

[21] W. Lukosz and R. E. Kunz, "Fluorescence lifetime of magnetic and electric dipoles near a dielectric interface," *Opt. Commun.*, vol. 20, pp. 195–199, Feb. 1977.

[22] W. Lukosz and R. E. Kunz, "Light emission by magnetic and electric dipoles close to a plane interface," *J. Opt. Soc. Amer.*, vol. 67, no. 12, pp. 1607–1615, Dec. 1977.

[23] H. C. Pocklington, "Electrical oscillations in wire," in *Cambridge Phil. Soc. Proc.*, vol. 9, 1897, pp. 324–332.

[24] N. K. Uzunoglu, N. G. Alexopoulos, and J. G. Fikioris, "Radiation properties of microstrip dipoles," *IEEE Trans. Antennas Propagat.*, vol. AP-27, pp. 853–858, Nov. 1979.

[25] I. E. Rana and N. G. Alexopoulos, "Printed wire antennas," in *Proc. Workshop on Printed Circuit Antenna Technology*, (New Mexico State University, Las Cruces, New Mexico), Oct. 1979, pp. 30.1–30.8.

[26] I. E. Rana and N. G. Alexopoulos, "Current distribution and input impedance of printed dipoles," *IEEE Trans. Antennas Propagat.*, vol. AP-29, pp. 99–105, Jan. 1981.

[27] N. G. Alexopoulos and I. E. Rana, "Mutual impedance computation between printed dipoles," *IEEE Trans. Antennas Propagat.*, vol. AP-29, pp. 106–111, Jan. 1981.

[28] I. E. Rana, N. G. Alexopoulos, and P. B. Katehi, "Theory of microstrip Yagi-Uda arrays," *Radio Sci.*, vol. 16, no. 6, pp. 1077–1079, Nov.–Dec. 1981.

[29] P. B. Katehi and N. G. Alexopoulos, "On the effect of substrate thickness and permittivity on printed circuit dipole properties," submitted for publication *IEEE Trans. Antennas Propagat.*

[30] P. B. Katehi and N. G. Alexopoulos, "On the theory of printed circuit antennas for millimeter waves," in *Sixth Int. Conf. Infrared and Millimeter Waves Dig.*, Dec. 1981, pp. F. 2.9–F. 2.10.

[31] P. B. Katehi and N. G. Alexopoulos, "On the nature of the electromagnetic field radiated by a printed antenna on a grounded substrate," UCLA Integrated Electromagnetics Lab. Rep. no. 3, 1981.

[32] D. B. Rutledge and M. S. Muha, "Imaging antenna arrays," *IEEE Trans. Antennas Propagat.*, vol. AP-30, pp. 535–540, 1982.

[33] D. B. Rutledge, D. P. Niekirk, and D. P. Kasilingam, "Integrated-circuit antennas," in *Infrared and Millimeter-Waves Series*, vol. 11, K. J. Button, Ed. New York: Academic, (to be published).

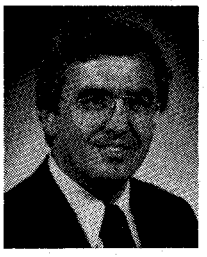

Nicolaos G. Alexopoulos (S'68–M'69–SM'82) was born in Athens, Greece, in 1942. He received the B.S.E.E., M.S.E.E., and Ph.D. degrees from the University of Michigan, Ann Arbor, in 1964, 1967, and 1968, respectively.

He is currently a Professor of Electrical Engineering at the University of California, Los Angeles, where he established the Integrated Electromagnetics Laboratory. His research interests are in the areas of integrated microwave and millimeter-wave antennas and circuits, optics, and electromagnetic scattering.

Pisti B. Katehi (S'83) was born in Athens, Greece, in 1954. She received the B.S.E.E. degree from the National Technical University of Athens in 1977, and the M.S.E.E. degree from the University of California, Los Angeles, in 1981.

She worked for the Naval Research Laboratory of Greece after receiving the master's degree, and is currently a graduate student in the Electrical Engineering Department, University of California, Los Angeles, pursuing the Ph.D. degree. She is a Research Assistant in the Integrated Electromagnetics Laboratory. She received the Amelia Earhart Fellowship, granted by the Zonta International Organization. Her research interests are in the area of integrated microwave and millimeter-wave antennas and circuits.

D. B. Rutledge (S'75–M'80) was born in Savannah, GA on January 12, 1952. He received the B.A. degree in mathematics from Williams College, Williamstown, MA, in 1973, the M.A. degree in electrical engineering from Cambridge University, Cambridge, England, in 1975, and the Ph.D. degree in electrical engineering from the University of California at Berkeley.

From 1975 to 1976, he was associated with the communications group of General Dynamics Corporation, where he worked with airborne microwave data systems. In 1980, he was appointed an Assistant Professor of Electrical Engineering at the California Institute of Technology, Pasadena, CA. He is working on millimeter and submillimeter devices and their applications.